Supplementary Information

Theoretical studies on excited-state properties of thermally activated delayed fluorescence molecules with aggregation induced emission

Yuzhi Song*, Bihe Li, Songsong Liu, Ming Qin, Yang Gao, Kai Zhang, Lili Lin, Chuan-Kui Wang, Jianzhong Fan*

Shandong Key Laboratory of Medical Physics and Image Processing & Shandong Provincial Engineering and Technical Center of Light Manipulations, School of Physics and Electronics, Shandong Normal University, Jinan 250358, China

Corresponding Author

*Author to whom correspondence should be addressed.

E-mail: fanjianzhongvip@163.com (J. Fan) and yzsong@sdnu.edu.cn (Y. Song).

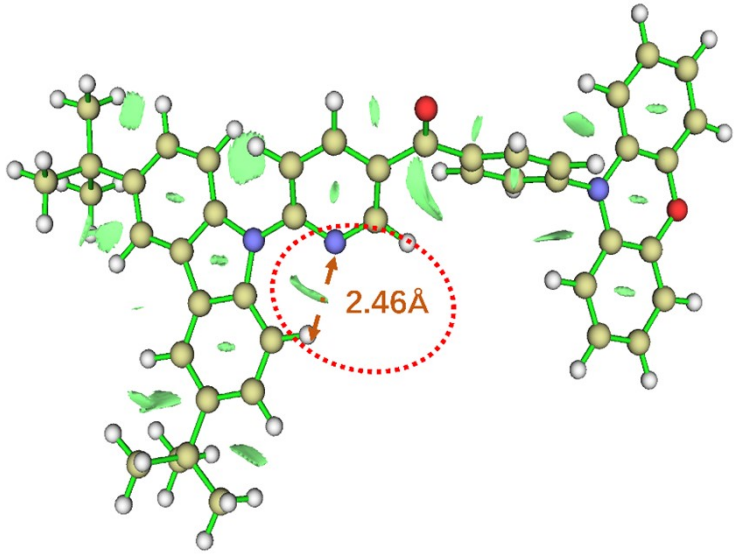

Figure S1. The visualization of intramolecular hydrogen bond between N and H (red circle).

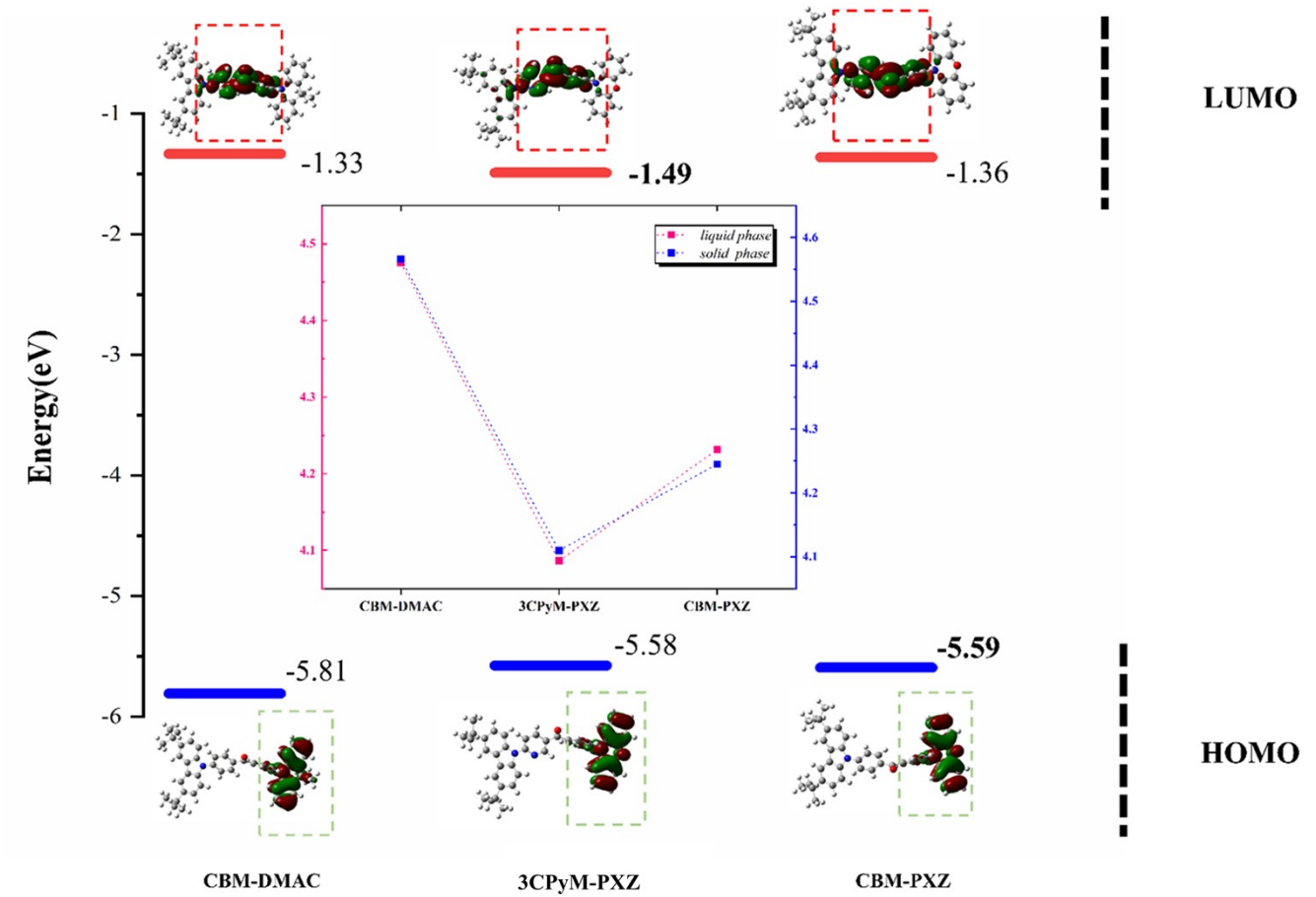

Figure S2. Energies and distributions of HOMOs and LUMOs for total molecules in THF. The interior illustration shows the energy gaps between HOMOs and LUMOs both in THF (pink line) and solid phase (blue line).

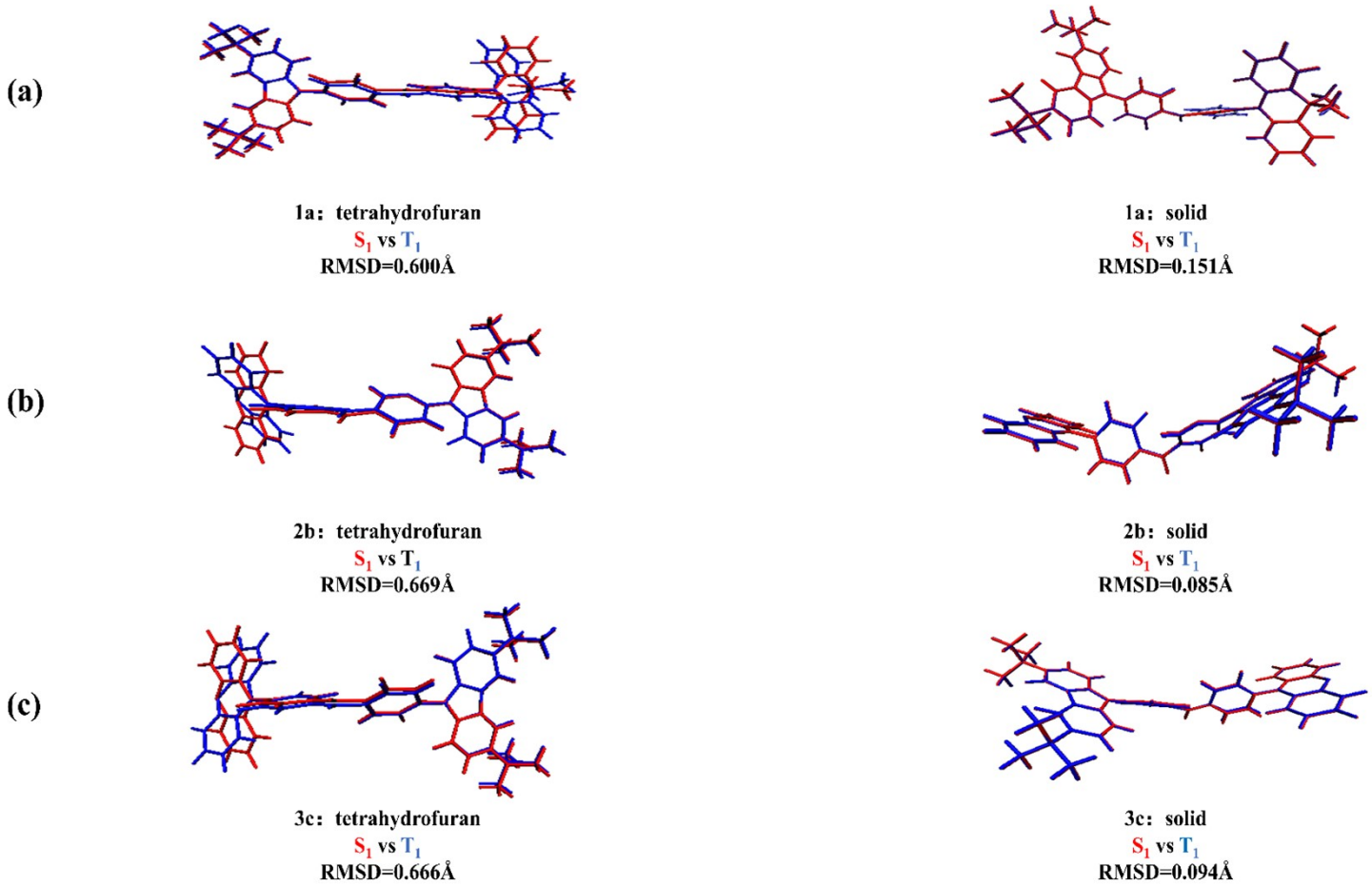

Figure S3. Geometry comparisons between S_1 and T_1 states in THF and solid phase for CBM-DMAC (a), 3CPyM-PXZ (b) and CBM-PXZ (c) respectively.

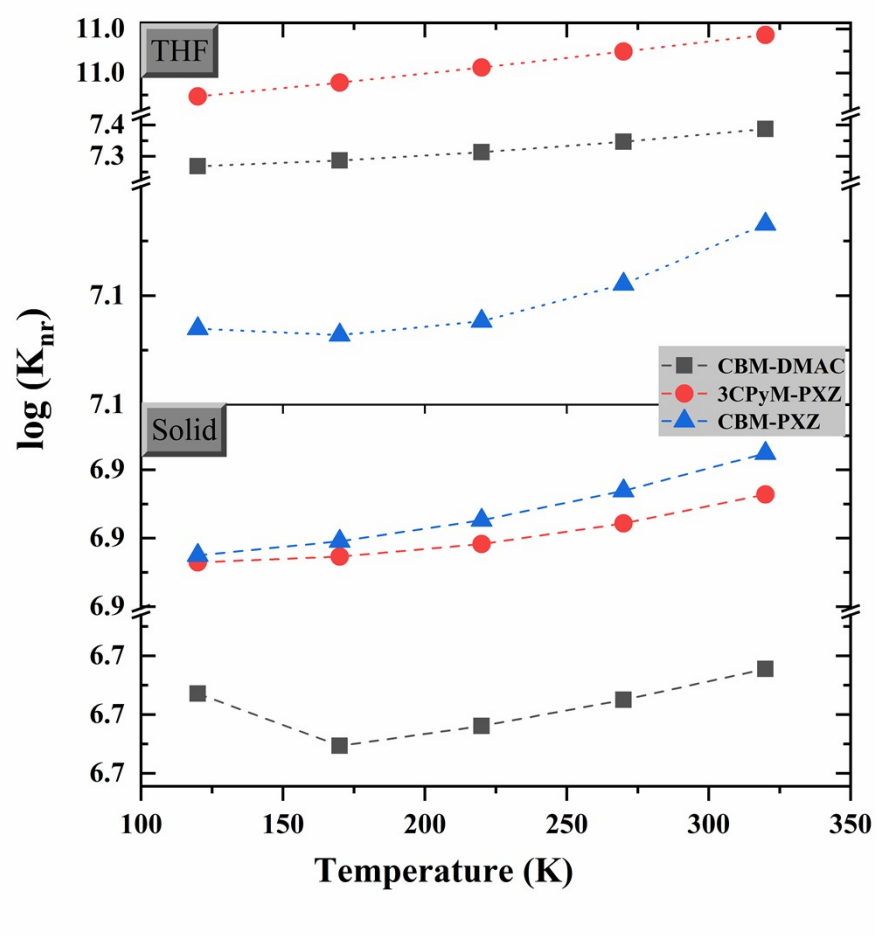

Figure S4. Temperature dependence of non-radiative decay rate for CBM-DMAC in solution and solid phase.

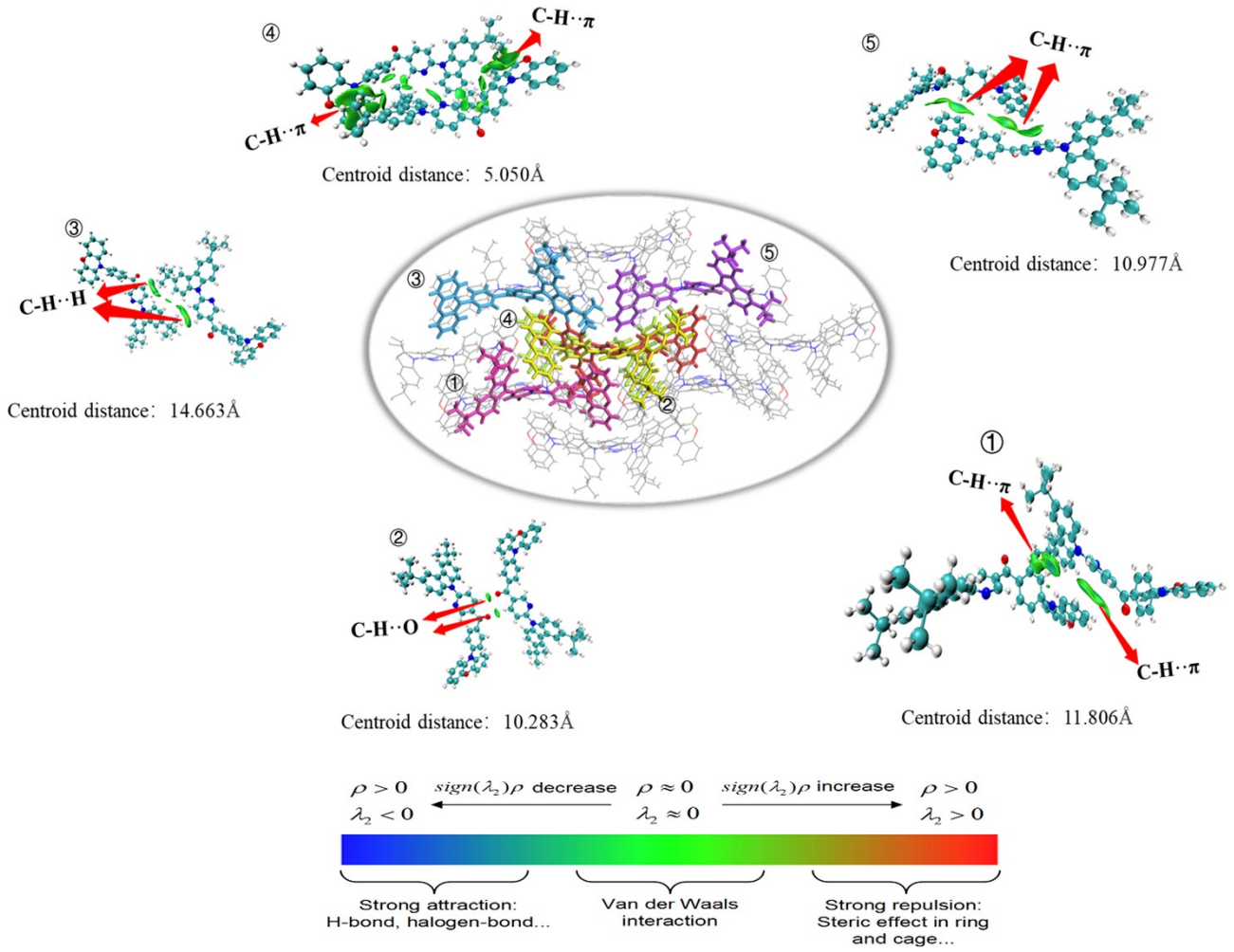

Figure S5. Intermolecular interactions and packing modes for several dimers from 3CPyM-PXZ crystal.

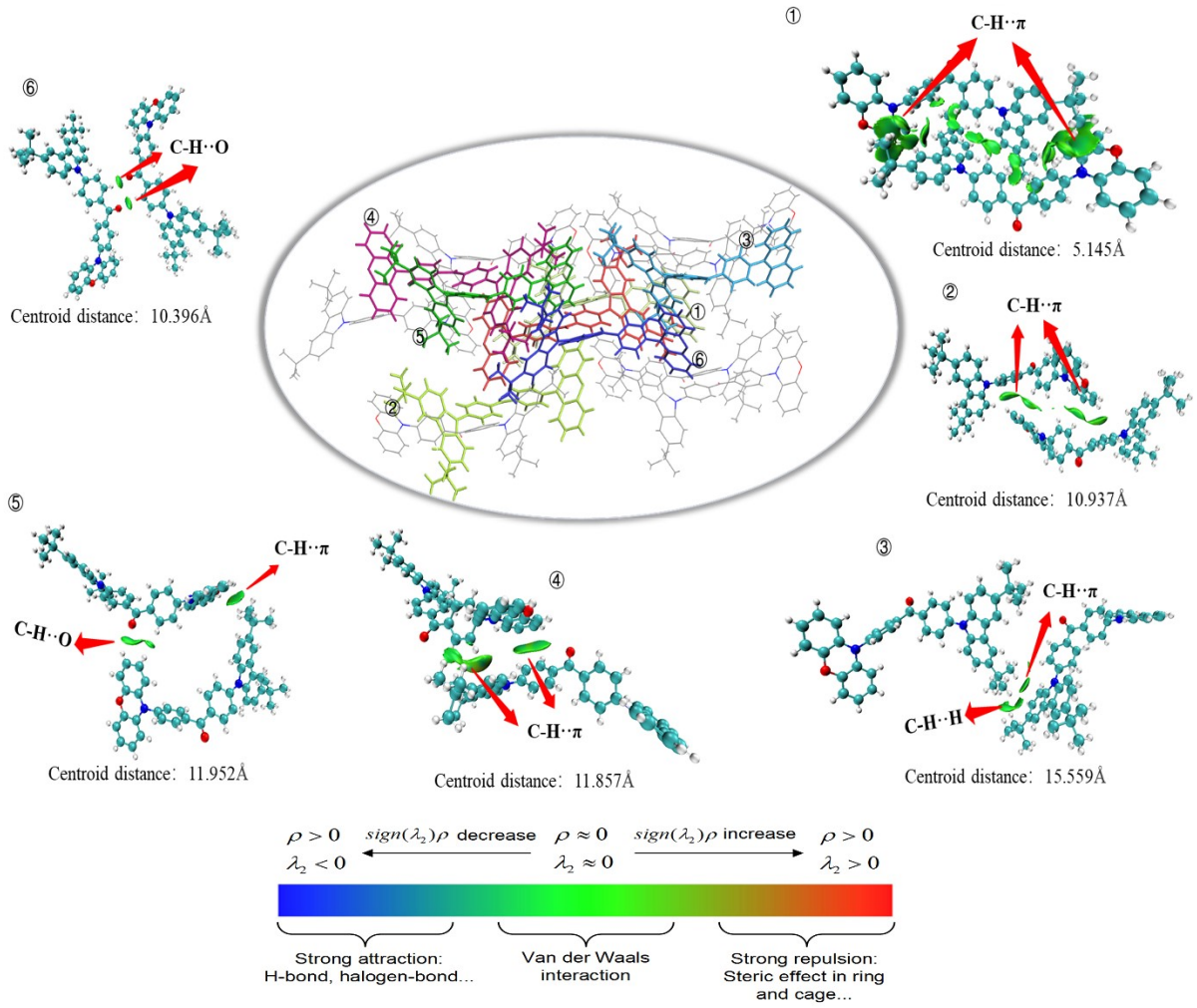

Figure S6. Intermolecular interactions and packing modes for several dimers from CBM-PXZ crystal.

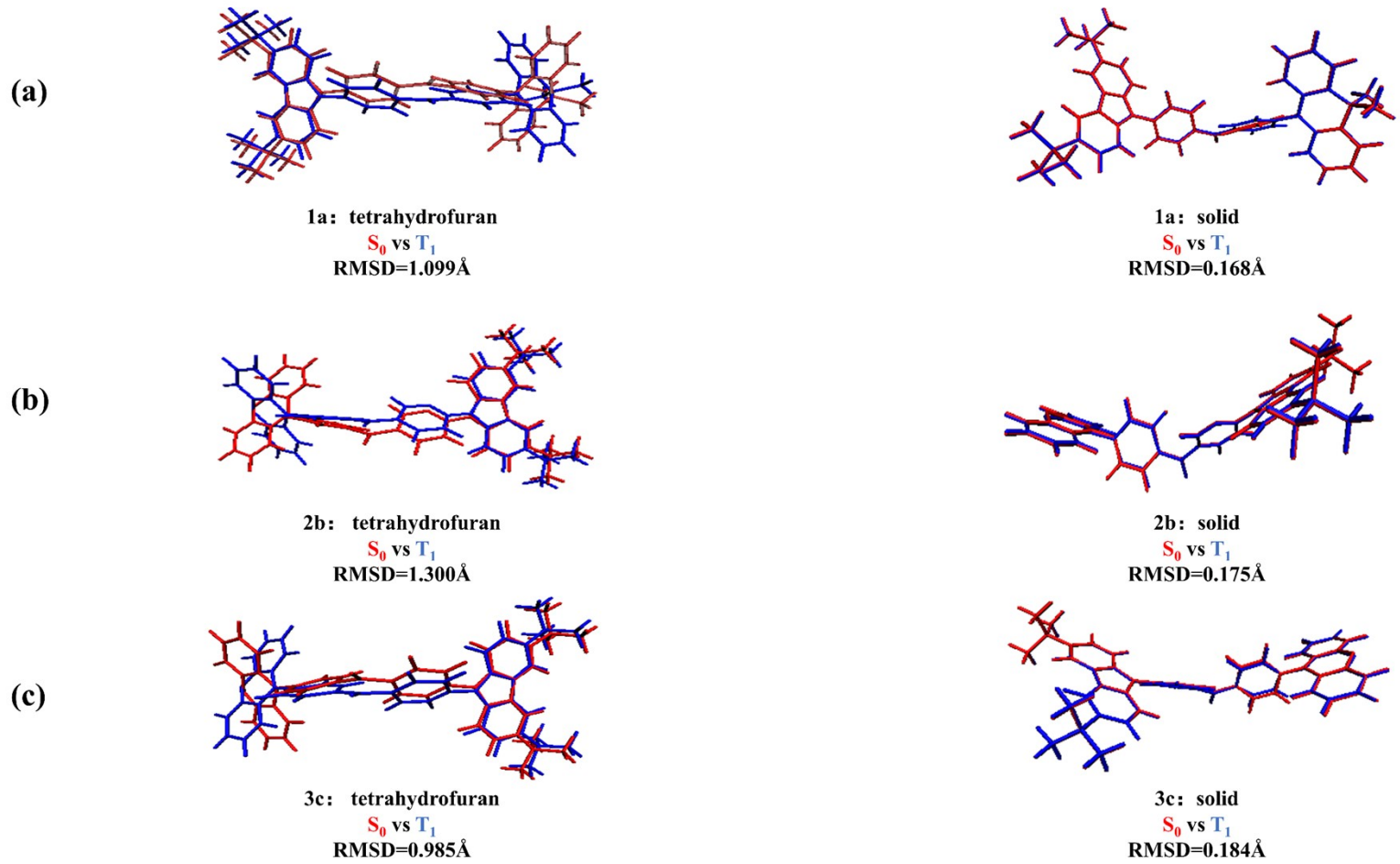

Figure S7. Geometrical changes between S_0 and T_1 states in THF and solid phase for CBM-DMAC (a), 3CPyM-PXZ (b) and CBM-PXZ (c), respectively.

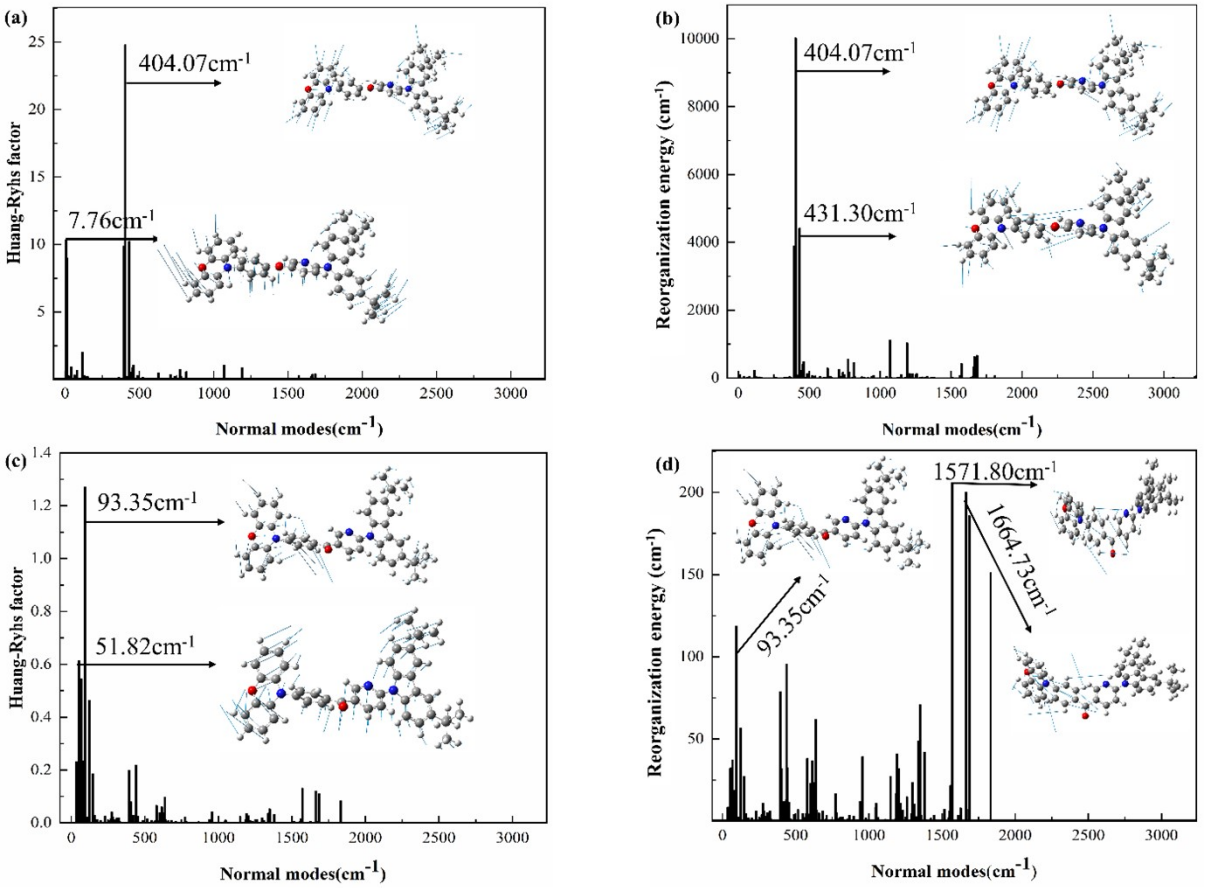

Figure S8. Calculated HR factors versus the normal mode frequencies in THF (a) and solid phase (c) as well as the reorganization energies versus the normal mode frequencies in THF (b) and solid phase (d) for 3CPyM-PXZ, respectively. Representative vibration modes are shown as insets.

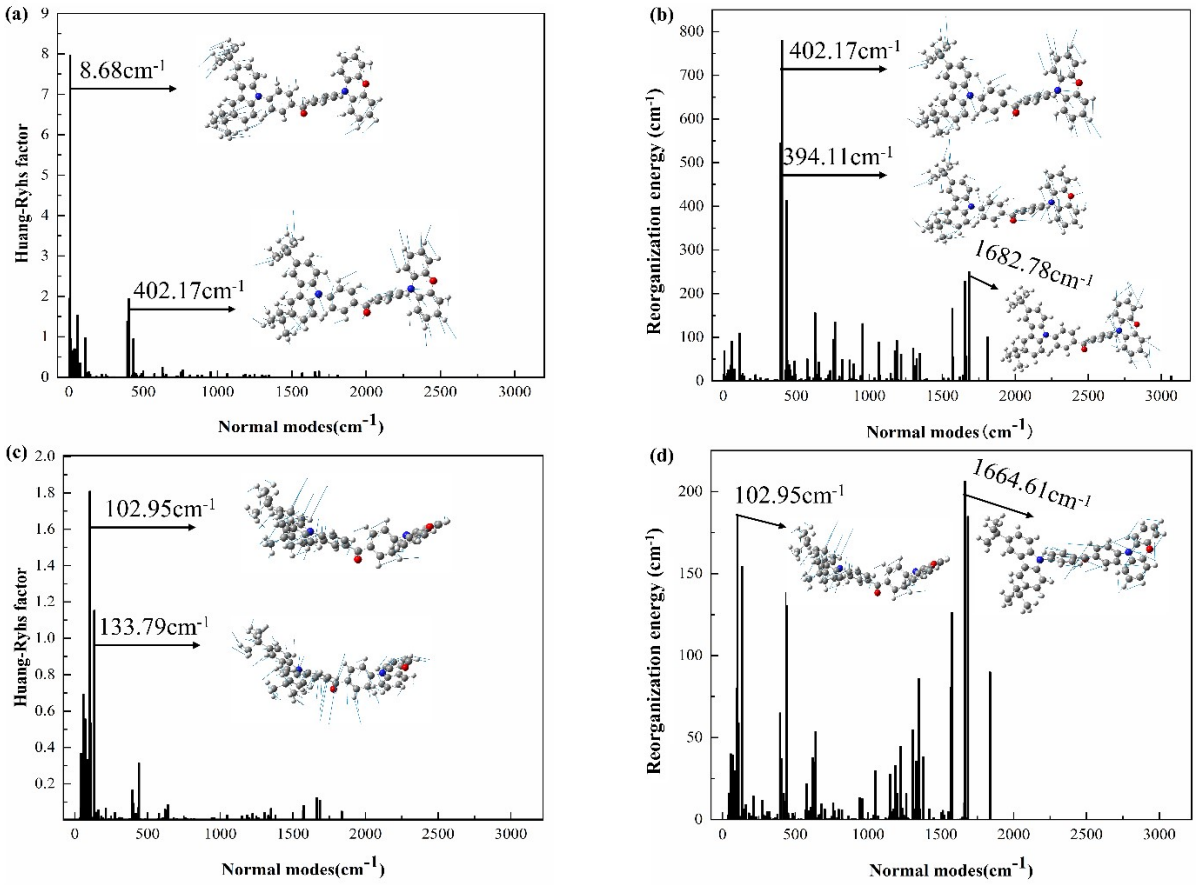

Figure S9. Calculated HR factors versus the normal mode frequencies in THF (a) and solid phase (c) as well as the reorganization energies versus the normal mode frequencies in THF (b) and solid phase (d) for CBM-PXZ, respectively. Representative vibration modes are shown as insets.

Table S1. Calculated reorganization energies of ISC and RISC processes between S_1 and T_1 for all molecules.

		λ_{ISC}(meV)	λ_{RISC}(meV)
THF	CBM-DMAC	154.93	227.93
	3CPyM-PXZ	84.41	187.25
	CBM-PXZ	99.59	191.69
Solid	CBM-DMAC	123.52	185.64
	3CPyM-PXZ	19.09	35.91
	CBM-PXZ	21.10	37.69

Table S2. Calculated oscillator strengths for all molecules.

		f
THF	CBM-DMAC	0.0006
	3CPyM-PXZ	0.0004
	CBM-PXZ	0.0006
Solid	CBM-DMAC	0.0270
	3CPyM-PXZ	0.0022
	CBM-PXZ	0.0004

Table S3. Calculated emission wavelength, adiabatic singlet (S_1) and triplet (T_1) energies and the orbital energies of HOMO and LUMO.

		λ_{em} (nm)	**S_1 (eV)**	**T_1 (eV)**	**HOMO (eV)**	**LUMO (eV)**
THF	CBM-DMAC	455.07	2.99	2.83	-5.81	-1.33
	3CPyM-PXZ	536.67	2.62	2.53	-5.58	-1.49
	CBM-PXZ	520.74	2.70	2.59	-5.59	-1.36
Solid	CBM-DMAC	445.74	3.03	2.84	-5.90	-1.34
	3CPyM-PXZ	555.75	2.51	2.47	-5.63	-1.52
	CBM-PXZ	530.02	2.62	2.59	-5.57	-1.32

Table S4. Calculated emission wavelength (nm) and radiative decay rate (s^{-1}) corresponding to different dihedral angles for CBM-DMAC in THF.

		20°	60°	100°	140°	180°
$\theta 1$	S_1	375.01	383.68	385.56	380.85	363.39
	K_r	9.49×10^4	4.53×10^4	4.49×10^4	9.20×10^4	3.54×10^5
$\theta 2$	S_1	382.35	346.24	336.34	370.49	389.45
	K_r	9.13×10^4	6.07×10^6	3.14×10^8	3.40×10^5	8.80×10^4
$\theta 3$	S_1	372.57	379.48	381.58	376.19	372.46
	K_r	3.36×10^5	1.39×10^5	4.58×10^4	1.41×10^5	1.44×10^5
$\theta 4$	S_1	337.68	362.42	360.37	354.38	334.44
	K_r	6.38×10^8	1.51×10^8	3.08×10^5	1.82×10^8	5.83×10^8

Table S5. Reorganization energies obtained by both AP and NM methods for total molecules in solid phase.

		S_0(meV)	S_1(meV)	S_0+S_1(meV)
CBM-DMAC	AP	254.70	268.91	523.62
	NM	245.95	307.38	553.33
3CPyM-PXZ	AP	274.29	437.89	712.18
	NM	307.85	548.84	856.69
CBM-PXZ	AP	279.68	452.21	731.90
	NM	322.14	530.61	852.75